3-2006

A Climatological Study of Equatorial GPS Data and the Effects on Ionospheric Scintillation

Katharine A. Wicker

A CLIMATOLOGICAL STUDY OF EQUATORIAL GPS DATA AND THE EFFECTS ON IONOSPHERIC SCINTILLATION

THESIS

Katharine A. Wicker, 2nd Lieutenant, USAF

AFIT/GSS/ENP/06-02

DEPARTMENT OF THE AIR FORCE
AIR UNIVERSITY

AIR FORCE INSTITUTE OF TECHNOLOGY

Wright-Patterson Air Force Base, Ohio

AFIT/GSS/ENP/06-02

A CLIMATOLOGICAL STUDY OF EQUATORIAL GPS DATA AND THE EFFECTS ON IONOSPHERIC SCINTILLATION

THESIS

Presented to the Faculty

Department of Engineering Physics

Graduate School of Engineering and Management

Air Force Institute of Technology

Air University

Air Education and Training Command

In Partial Fulfillment of the Requirements for the

Degree of Master of Science (Space Systems)

Katharine A. Wicker, BS

2nd Lieutenant, USAF

March 2006

AFIT/GSS/ENP/06-02

A CLIMATOLOGICAL STUDY OF EQUATORIAL GPS DATA AND THE EFFECTS ON IONOSPHERIC SCINTILLATION

Katharine A. Wicker, BS
2nd Lieutenant, USAF

Approved:

Steven T. Fiorino (Chairman)	date
Christopher G. Smithro (Member)	date
Richard G. Cobb (Member)	date

Abstract

Ionospheric scintillation is detrimental to radio signals, especially those from the global positioning system. Such scintillation is caused when a signal permeates the ionosphere through plasma bubbles. The signal's phase and amplitude can be altered, and a receiver on the ground can lose lock on the GPS signal. Measured using a zero to one index known as S4, scintillation severity is based upon season, solar cycle, time of day, location and frequency. The most severe scintillation occurs at the equatorial anomaly, or fifteen degrees north and south of the equator. Seven years of data from fifteen different locations around the equator were used in a Matlab program to determine if the current trends still apply. Previous research has found the S4 at the equator to peak during the months of September to March, between the hours of 2000 and 0300 local time, and when the sunspot number is above 60. Matlab plots were generated to find peaks in scintillation based upon location and month. These were compared to sunspot numbers during those months. A new Matlab program was made to compile all of the plots into a climatological map of the seasonal data. Trends similar to those found previously were discovered. S4 numbers peaked in the area of the anomaly, and between the months of October to March. As the sunspot number increased, the yearly average scintillation also increased. The hours of 000 to 0300 GMT also saw a peak in S4 scintillation, which agrees with previous findings. This research showed that solar maximum years, the hours of 000 to 0300 GMT, and the months of October through March have the largest amount of scintillation.

To my parents and my husband

Acknowledgments

I would like to thank my advisor, Lt Col Steven Fiorino, my sponsor from AFRL, Dr. Keith Groves, and AFIT's computer expert, Dr. Charles Leakeas. Without their help, I would not have been able to complete this project. I truly appreciate their hard work and dedication.

Katharine A. Wicker

Table of Contents

List of Figures

List of Tables

A Climatological Study of Equatorial GPS Data

and the Effects of Ionospheric Scintillation

I. Introduction

Everyday, people use satellites to communicate with each other all over the world. As those communication signals pass from the user to the satellite and back again to the receiver station, many interruptions can occur. The ionosphere of the earth, or the ionized gas region of the atmosphere, is very important to radio communication. However, the ionosphere can also contain plasma bubbles that make signals fluctuate and cause accuracy problems with the Global Positioning System.

In the earth's ionosphere, or between 80 and 1500 kilometers above the earth's surface, there exists a phenomenon known as scintillation. Scintillation is the rapid fluctuation of the phase and intensity of a radio signal as it is transmitted through plasma density irregularities in the earth's ionosphere. This is very common with signal-to-ground propagation channels. (Parkinson)

Scintillation by itself does not affect anything, but when coupled with the Global Positioning System, problems may arise. The constant fluctuations interfere with the GPS accuracy as the radio waves also pass through the earth's ionosphere. Scintillation results in signal power fading, phase cycle slips, and loss of satellite lock.

Currently, there are few records of outages for GPS users in the equatorial region of the world, so when an outage occurs, the user has no idea if the problem is due to their equipment, their environment, or their enemy. Through this research, we will be able to predict and help assess future GPS scintillation impacts.

This thesis, statistically determines a climatological pattern of GPS data collected at the equatorial region of the world. Expected is a definite pattern present based on the season, yearly average and time of day. If a pattern is found, this would greatly aid GPS capabilities in the future. Such errors could be subtracted from the current data based upon the seasonal or yearly pattern developed.

This academic effort will focus on four main areas. First, there will be a literature research, where previous Global Positioning System and scintillation work will be discussed in detail, and how they may affect this topic. Second, will be the methodology used to determine a climatological pattern using FORTRAN, Matlab, and Access, and as statistical and climatological tools to interpret the data. Third, the raw results will be presented for the basic overall pattern depending on month and solar cycle. Fourth and lastly, the conclusion will discuss how these patterns can be used.

II. Literature Review

General Issue

When using the Global Positioning System, many different topics must be understood before one can determine the accuracy of the signal. First, the basics of GPS, how the system bands are used, and how the entire system works together must be explored. Second, the idea of total electron content, differential GPS, and degree-of-precision are keys to understanding the current problem. Third, the scintillation problem and multipath ideas are discussed to round out the problem description. Once all of these areas are covered, the effect of ionospheric scintillation on the GPS data can be determined.

Global Positioning System

GPS consists of a number of satellites that transmit precisely timed GPS signals at two L band frequencies, at 1.57542 GHz (L_1 band) and 1.2276 GHz (L_2 band). These bands, along with L_3 band at 1.38105 gigahertz were selected and filtered as to minimize interference with the radio astronomy bands. The L bands also give acceptable received signal power, reasonable satellite transmit power levels, and earth coverage satellite patterns. By using both the L_1 and L_2 bands, the dual frequency allows for ionospheric corrections and ionospheric group delay measurement. In general, GPS signals have different perturbations due to the specific L bands used. These bands were selected for their ability to limit the ionospheric delay effects. However, the elevation angle and environment the signal traverses causes scintillation to persist. (Parkinson)

Each GPS signal has imbedded navigational data composed of the precise satellite clock time and the satellite's position. The user can then determine the satellite's time and position at time of transmission. This navigational data is uploaded, via S-band telemetry, to each satellite from the GPS control segment, and then stored in memory in the satellite for readout. Each control segment also uploads the satellite orbit, exact position in that orbit versus time, and a satellite clock correction. This correction calibrates the offset of the satellite clock relative to the GPS system time. (Parkinson)

Each GPS has a satellite based augmentation system. They are used for navigation and precision approach that allows GPS to achieve good accuracy. Each SBA currently has a delay locked loop (DLL) or phase locked loop (PLL) installed to give users the ability to handle moderate scintillation. While DLL/PLL helps with some scintillation around the equator, a better system must be developed to predict and subtract the damaging effects. (Parkinson)

Today there are about 360 global positioning system, or monitoring, stations worldwide. “Each receiver at these stations is capable of receiving L-band dual frequency signals from 8+ GPS satellites simultaneously in different directions.” (http://iono.jpl.nasa.gov/scint.html) GPS data is now being used to measure and detect ionospheric scintillation effects. The signal phase fluctuation is measured, and then classified by the total electron content (TEC) index. The TEC index is used to show the difference between quiet time ionospheric variations and fluctuating times. One unit of TEC i.e. 1x10^16 el/m^2, introduces a range error of 0.16 m at the L1 1.6 GHz frequency of GPS. During these non-quiet times, the GPS signal can become degraded. (http://www.nwra-az.com/ionoscint/)

The fading of GPS signals is caused by variations in ionospheric total electron densities, which produce a statistical decrease in satellite variability. Pseudorange errors can also occur because of signal delays, or the TEC, for the signal path of the satellite. "The difference between satellite clock time and user clock time when the user clock is not precise is termed psuedorange" (Parkinson). These errors are from reference receivers that determine pseudorange errors that will be sent to other nearby receivers. These errors can disturb, or scintillate, the phase and amplitude of radio signals that pass through the ionosphere. The phase of a radio signal refers to its' direction, and the amplitude refers to the radio signal's height. If either of the phase or amplitude is altered, the receiving station does not know from where the signal originated (Parkinson).

Another type of GPS is differential GPS, or DGPS. "If two GPS receivers operate in relatively close proximity (less than 100 km), many of the errors inherent in two GPS position solutions are common to both solutions." (Parkinson) The difference between the two can cause problems with the satellite clock time, or ionospheric error to arise. Such errors can usually be fixed by knowing the location of one of the receivers. That receiver will then transmit correction information to other neighboring receivers, thereby increasing the level of accuracy for the other users. Basically, each reference station transmits corrections for each satellite in view on a separate radio frequency carrier, or a pseudorange. This correction data also includes an almanac giving locations of other DGPS reference stations, so that users can choose the one closest to their current location. The DGPS system is limited to users and reference stations about 100 kilometers apart. Wide area differential GPS, or WADGPS, can also be used in cases where the distance is

too great, to use normal DGPS. (Parkinson) The basic differential global positioning system can be seen in Figure 1 below.

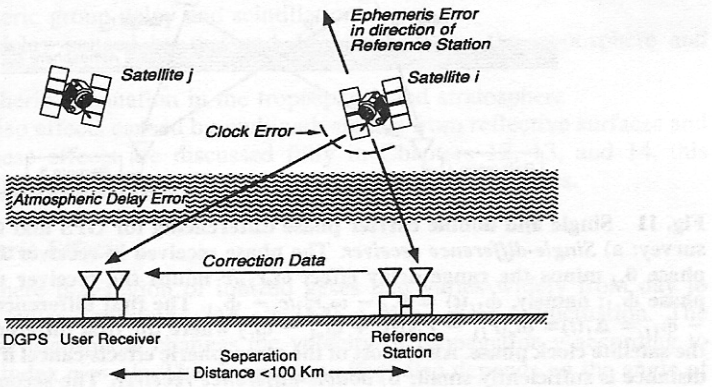

Fig.1 **Simplified view of differential GPS. This correction can completely eliminate satellite clock error offsets but ephemeris and atmospheric corrections differ for the user from the reference station by an amount that depends on the separation distance.**

(From Parkinson)

Figure 1. Differential GPS

Ionosphere

The ionosphere is a layer of the atmosphere full of ionized gases. The amount of gas present depends on the day, time, season, and solar cycle. These same criteria apply to the fluctuation of scintillation, due to its ionospheric origins. These gases cause a change in how fast the signal passes though the ionosphere, or propagation velocity, and are also dependent on the incident angle of the signal. Most of the ionosphere's electron content is located 200 to 400 kilometers above the earth's surface, and fluctuates from day to night. Unlike the troposphere, the refractive index, or n=c/v, where n is the refractive index, c is the speed of light, and v is the propagation velocity, changes with frequency. Since this varies, group delay, carrier phase advance, and scintillation occurs. (Parkinson)

Group delay and carrier phase advance are dependent on signal path and the amount of electron density the signal encounters. The group delay of a signal is directly proportional to its ionospheric TEC. The carrier phase is calculated from equations that involve receiver pseudorange measurements, and the L1 and L2 frequencies. Scintillation, on the other hand, has been found to change the phase and amplitude of the signal with respect to time. Group delay, phase advance, and scintillation all depend on the frequency of the received signal. Ionospheric delay is equal to vertical TEC over the frequency squared, so the dual frequencies measured at L_1 and L_2 bands can be used to calculate the delay.

Ionospheric Delay = Vertical TEC / (frequency)^2 (Equation 1)

Faraday rotation and ray bending also change how long it takes a signal to traverse the ionosphere, but they are not relevant to this scintillation study due to their minor effect. (Parkinson)

Scintillation

Scintillation is caused by radio signals traversing through plasma irregularities in the ionosphere. The formation of these bubbles is caused by the Rayleigh-Taylor Instability, which creates a perturbation. These form on the underside of the F2 ionospheric layer, and become larger at the magnetic equator. The F2 layer of the atmosphere is located 250 to 500 kilometers above the surface of the earth. It is known as the dominant reflecting layer of the ionosphere, so signals that encounter this region may have a delayed transmission. The aforementioned perturbations produce a bubble of

depleted ionization that continues to move to higher altitudes. Over time, this breaks down into smaller irregularities that continue down the magnetic field lines. These bubbles cover a number of scale sizes that make up a random diffraction screen for any signal passes through. (Thomas)

One way to scintillate and effect GPS is with multipath signal reflections. Multipath signal reflections and ionospheric variations effect differential GPS or DGPS in different ways. Differential GPS has a receiving end of the signal is that is stationary, while the transmitting end moves. This results in two different frequencies to find timing errors, which causes propagation effects. However, DGPS is still prone to scintillation, which cannot be removed. In 1996, Bruce Nordwall researched this topic and found a lower output from the current satellites and problems during solar cycle peaks. At the time, manufacturers were making GPS receivers to receive the current strength, but the satellites were specified for a lower level. Therefore, manufacturing differences could lead to a power difference of a few decibels. (Nordwall)

The equatorial electrojet causes some of the problems observed at the equator. Since the magnetic field at the earth's equator is horizontal, the flow around the equator is altered based upon time of day. During the day, energy flows eastward, and at night it flows westward. (Tascione)

In the F region of the ionosphere, plasma convection occurs to further support the irregularities encountered in this project. Plasma flows up and westward during the day, and down and eastward at night. In the daytime, the plasma is brought up to higher latitudes where more plasma can be reproduced. This phenomenon is due to slow recombination at these latitudes. An increase in the plasma production makes ionization

peaks around the equator, known as the equatorial anomaly, or the fountain effect. (Tascione)

For a large portion of the areas analyzed, their results can be attributed to the South Atlantic Anomaly and the Southeast Asian Anomaly. The South Atlantic Anomaly is due to the earth's tilted geomagnetic field. This field does not line up with the geographic equator, so the radiation belts are close to the South Atlantic area of the world. Trapped particles in these belts go to lower altitudes, where they interact with neutral, and cause further F region irregularities. The Southeast Asian Anomaly is responsible for the D region absorption in this area due to higher energy particles being present. (Tascione)

Many different factors contribute to the scintillation fluctuation, but the main cause is spread F. A nighttime equatorial occurrence, this F region anomaly can last anywhere from a few minutes to several hours. It is caused by turbulence that alters electron density in the ionosphere. The F region becomes fatter than normal, and can distort radio waves. Some researchers believe spread F to be caused by buoyancy factors. This is due to low ion dense areas moving up to create waves.

> "When the waves move upward, steep density gradients along the edges can become the source of smaller scale irregularities which produce intense distortion of gigahertz frequency radio waves." (Tascione) (see figure 2 below)

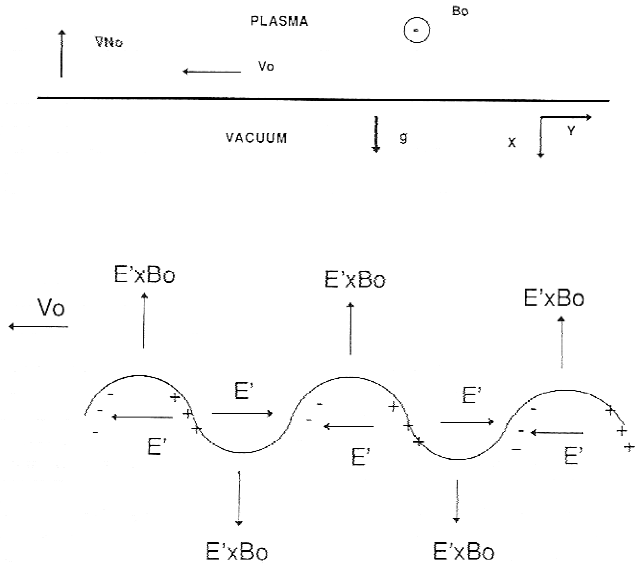

Figure 2 a) Sketch showing the idealized conditions in the low-latitude F-region after sunset (no E- or F1-regions); (b) the physical mechanism of the $\vec{E}' \times \vec{B}$ gradient drift instability *(after Keskinen, 1984)*.

Figure 2. Ionospheric plasma flow

The ionosphere can do one of four things to a radio wave. First, it can attenuate the signal, or amplify it. This is done by taking energy from the wave using charged particles. Secondly, the ionosphere can limit, or decrease the signal's range. Limiting is accomplished by absorbing the wave's energy. Third, the ionosphere can change the direction of the wave by altering the electromagnetic density. Lastly, the region can reflect the radio wave away from its' intended target. While each of these cause problems for Global Positioning System users, the one that limits the downrange distance is the most severe problem at the equatorial anomaly.

Scintillation Trends

Normally, ionospheric variations are not a problem at GPS frequencies and in mid latitudes, but there is a problem during solar maximum. "Scintillation effects are greatest in the several years at the peak levels of the eleven year solar activity (sunspot) cycle.

(Bishop 1, 1994). "It seems likely that the ionosphere will have some important impacts on GPS at solar maximum, both link outages due to scintillation, and navigation errors due to large-scale structures." (Nordwall, 1996). Many experts use this critical information to focus their research only on the solar maximum periods.

"The severity of scintillation varies with frequency, location, time of day, season and sunspot cycle." (Bishop 1, 1996). However, certain aspects are known about the scintillation effects at the earth's equator. The effects decrease as frequency increases, and the equator at solar maximum causes these problems to arise more often.

Scintillation itself is actually estimated in terms of power spectral density of phase. The frequency of the wave, a strength parameter, and a unitless slope variable are all entered into an equation to determine S4 index. S4 is calculated using Equation 2 below, where I is the signal intensity. (Fu)

$$S4 = \sqrt{(\langle I^2 \rangle - \langle I \rangle^2) / \langle I \rangle^2} \qquad \text{(Equation 2)}$$

Since scintillation is a function of solar cycle, time of day, time of year, and location, it is not possible to plot all these factors on one plot. S4 was developed to create a wider understanding of the amplitude fading in a certain area. A value of zero for S4 means no scintillation, and a value of one means severe scintillation. (Parkinson)

Scintillation can cause severe fades in a radio signal or phase gradients that decrease a user's chance of "locking" onto a signal. The GPS satellite signals can also have data loss, which may cause a decrease in signal performance or tracking capabilities. When the earth is experiencing solar maximum, significant disturbances can

occur to the GPS system. At solar maximum, the ionosphere has lower or higher regions of electron densities, so this greatly affects the GPS, especially near the equatorial anomaly. The equatorial anomaly region, which consists of two belts, several degrees wide, and fifteen degrees north and south of the equator, is the region of the worst scintillation in the world. This unique region of the world experiences fading up to twenty decibels during the hours of 2000 to 2400 local time. (Groves)

Scintillations primarily occur during the few hours before midnight, and can last until after midnight during geomagnetic storms, or when the Kp index is higher than one. Kp is a three hour geomagnetic planetary index that is based upon the K index that has 12 stations around the world. Among their research conducted on equatorial GPS data, the scintillation peaks were found to vary up to twenty decibels, and the signal level often faded three decibels or more. The lab also found that changes experienced on days without noticeable scintillation, or quiet day oscillations, are due to multipath errors. (Knight)

Multipath effects are another type of interference common with GPS. "They occur when satellite signals reflected from surfaces near the receiving antenna interfere with the direct satellite signal." (Nordwall, 1996). While multipath effects are always in the atmosphere, they cause the most havoc for the high precision DGPS, and also make up the largest source of error. (Nordwall)

Ionospheric fading, or scintillation, is determined by ionospheric domain and the system application used. When dealing with the ionosphere, researchers must consider the elevation angle of the satellite path. At lower elevation angles, ionospheric path lengths are longer, and the magnitude effect is also greater. As the atmosphere becomes

more disturbed, the fading of the radio signal increases. Phase rate errors can cause apparent changes in the frequency of more than one Hertz per second. This kind of shift makes the error outside of the tracking ability of most receivers. (Bishop 2)

As already stated, scintillation is dependent on geographical location. Severe cases are also seen in the polar and auroral regions of the world, but not with the strong fading experienced in the equatorial region. However, polar scintillation can extend to 1000 kilometers in diameter, which can affect more than one satellite at the same time. The major scintillation regions of the earth can be seen in Figure 3 below. This research is interested in the equatorial region only. (Bishop 2)

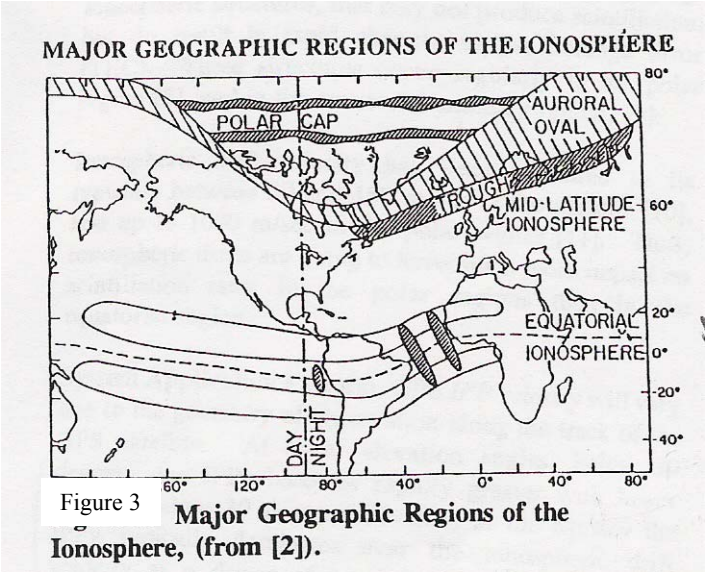

Figure 3. Regions of the Ionosphere

For GPS, ionosphereic scintillation can cause many problems. A reference station and navigation receiver could observe the same satellite with very different ionosphereic errors, and the location would be perceived to be higher or lower in altitude than it is in

reality. This is because vertical direction positioning can be influenced by one satellite's signal. (Parkinson)

Higher frequency signals are more likely to have a GPS outage due to ionospheric scintillation. Therefore, during strong scintillation, a dual frequency GPS user would first lose his ionospheric correction. This would cause a decrease in range accuracy, without the user even knowing it has occurred. (Bishop 1)

The dilution-of-precision, or DOP, uses pseudorange and positioning accuracy to determine the capability for GPS satellites. DOP is not the only means of determining positioning accuracy, but it is the most widely used. Position accuracy is similar to ranging accuracy by the direction of the satellite signal's arrival. To find a specific accuracy for positioning, the ranging accuracy and ranging geometry must be found. The unit vectors to each of the satellites are used to calculate the DOP, and if the value is greater than six, the satellite geometry is determined to be poor. (Parkinson)

While many other researchers have written on this topic, few have performed a climatological study of this sort. Bishop, Basu, Knight, Groves and other have established good overall trends for the region. Different researchers have agreed upon similar thresholds for the seasons, time of day, and solar cycle at the equatorial anomaly. The months of October to March have the greatest amount of scintillation in the equatorial anomaly region. Between the hours of 2000 and 0000 local time, the scintillation numbers are the greatest in this are. When the year is a solar maximum year, the S4 scintillation numbers are higher than solar minimum years.

Research Data

Currently, the Air Force Research Laboratory takes fifteen intervals of data for their scintillation network decision aid (SCINDA), which makes three dimensional tri-color maps of the world. Such maps are used by scientists to better understand how scintillation structures develop, and also by operators to find practical ways to maintain good communication. All of the AFRL's SCINDA data is used to create predictions for scintillation regions of interest. SCINDA data is available from eleven locations worldwide which includes scintillation data (or S4) and ion drift velocities from available satellite links. (www.vs.afrl.af.mil)

The locations selected for use in this project were done so due to their geographical locations. All of the receiver stations are in the equatorial anomaly band that is 15 degrees north and south of the equator.

Scintillation Classification System

In 1994, Hajkowski conducted a study of scintillation at sunspot maximums, and developed a classification system for all regions of the globe. The three different types found are N, P, and S types. The N type is defined to occur north of the equatorial boundary. The P type occurs at the equator and is due to the electrical density irregularity patches that bend the signal in the ionosphere. Each patch is made of rod shaped field aligned irregularities (FAIs), that are associated with F2 layer disruptions. This type of scintillation occurs most often during the nighttime or during the maximum in spread F occurrence at solar minimum. S type scintillation occurs at the equatorial edge of the auroral scintillation belt. This type causes the worst of the scintillation at the mid-latitude stations. S type scintillation is correlated to a peak in the 10.7 cm solar radio

flux that occurs at solar maximum. During the summer daytime S type is found to occur due to sporadic E. Sporadic E is a regular daytime occurrence in the equatorial regions fo the world that peak in early springtime and summer. (Hajkowski)

Summary

In summary, scintillation wreaks havoc at the equatorial anomaly based upon season, time of day, frequency, and solar cycle. The months with the most scintillation in the southern hemisphere are September to March. (Bishop) The most scintillation is also found between the hours of 2000 to 0300 local time, or from sunset until before sunrise. For frequency, as it increases, the scintillation increases. Lastly, scintillation is the greatest during the peak of a solar cycle, or when the sunspot number is greater than sixty.

By understanding the basics of GPS, and the problems that the earth's ionosphere poses to satellite signals, we can pursue our climatological study of the data. While most of this research has not been done before, many thresholds will be referenced for comparison. The GPS and the earth's ionosphere require a correction system for the equatorial anomaly region, so one must be developed for the part of the sky covered by the scintillation problems.

III. Methodology

Overview

The methodology for this thesis will include FORTRAN, Access, and Matlab programs that will provide a climatological study of the ionosphere's effect on the global positioning system's data collected at locations around the earth's equator. For each satellite, the data was recorded using Universal Time (UT) with corrected S4 in the range of zero to one. Scintillation found to be larger than one was attributed to multipath propagation, and was ignored for this project.

FORTRAN Program

First the data was put into a FORTRAN program that separated the data into seven distinct columns. The areas of interest were the year, date, time, S4 scintillation number, satellite latitude, satellite altitude, and satellite longitude. If the S4 scintillation number is equal to 9.999, the data is an error value and the FORTRAN program deletes this value. Our research was not concerned with the satellite's altitude since all of these numbers were between 4.1 and 4.2 kilometers. These small differences were enough to ignore the altitude factor for our equations. Instead, we focused on three main areas of interest. First, we took the day of the year to create maps of the worst scintillation months of each year. Second, we used the time of day, to create maps of the worst scintillation times of day. Third, we used sunspot number tables to determine if solar cycle had any effect on the S4 data collected around the world.

Monthly Data Compilation

To determine the worst scintillation months of the year, a specific Matlab program had to be generated. The files were separated into years, and then into months.

The data was not originally sorted by month, so I determined the days of each year from 1997 until 2004, and put each file into its appropriate month folder. (see Table 1 below)

Table 1. Days of the Year

Days of the Year		
Month	Non Leap (97,98,99,01,02,03)	Leap (00,04)
Jan	1 to 31	1 to 31
Feb	32 to 59	32 to 60
Mar	60 to 90	61 to 91
Apr	91 to 120	92 to 121
May	121 to 151	122 to 152
Jun	152 to 181	153 to 182
Jul	182 to 212	183 to 213
Aug	213 to 243	214 to 244
Sept	244 to 273	245 to 274
Oct	274 to 304	275 to 305
Nov	305 to 334	306 to 335
Dec	335 to 365	336 to 366

Since I did not know how to create a script to automate file loading, I needed a way to load the data. I could either individually load each file for each month, which was sometimes more than fifty files, or I could assemble one large file for each month of each year. I choose the later, and began making large text files for each month of each year. This task alone was a great deal of work, since each month had at least twenty files, and there were eight years worth of data. After compiling a file for each month of each year, I was able to load one file at a time and use a specific Matlab program to create 'meshgrid' plots of the S4 data based the month of the year.

Previous research did not focus on each month individually, but rather on seasons of the year. I then divided each year into four seasons that fell January to March, April to June, July to September, and October until December. This data will henceforth be referred to as seasonal data in the next two chapters.

Yearly Data Compilation

The data from the eleven different equatorial locations were already divided into years, so I found the average and standard deviation for each year. The results of these calculations can be found in Table 10 in Chapter 4.

Hourly Data Compilation

Next I tackled the time of day issue for the data. I created a Matlab program that sorted the data according to time of day. The time in the data is all recorded in seconds in Zulu time, or Greenwich Mean Time. These times were adjusted for local time.

For our purposes, I ignored the elevation angle for the data analysis. While the elevation and azimuth angles do affect how much of the ionosphere the radio signal must traverse, it was beyond the scope of this research endeavor.

I then proceeded to import the data into Access. Access is a database program that is part of the Microsoft Office package. Each month's data was imported and the S4 column was sorted into useful and non-useful data. All of the useful S4 data had to be between zero and one, and not be an error value of 9.999 or 9.990. By using Access to run a query of all S4 data lines less than one, I was able to circumvent Matlab code and find the data I needed to later import into Matlab. Once each month's usable data was assembled, the lines of data with 9.990 or 9.999 were deleted. This final product was then imported to Matlab to create a multicolor 2D plot of the the S4 data based upon

latitude and longitude. Each location has one plot for each month, one plot for each hour of the day, and one plot for each year's solar minimum and maximum. All of the eleven locations are referred to in the data by a 2-letter abbreviation. These abbreviations were provided by the AFRL researchers who collected the data. (see Table 2 below)

Table 2. Site Name Abbreviations

Site Name	Abbreviation
Ancon	GB
Antofagasta	GA
Asccension	GE
Bahrain	GG
Darwin	GF
Diego	GH
Fang	GX
Guam	GC
Parepare	GW
Pontianak	GY
Vanimo	GZ

Statistics

After all S4 values greater than one and errors have been removed, statistical values can be determined. Values greater than one were found, and since S4 is a zero to one index, any number greater than one is assumed to be an error value. First, Matlab was used to find the arithmetic mean of each month for each location for each year. The mean is a statistical value equal to $(\Sigma x_i)/N.$, or the sum of all the values divided by the number of values. Second, Matlab was also used to calculate the standard deviation from those means for each month for each location for each year. Standard deviation is a commonly used measure of variation that tells how far from the mean your values are located. Standard deviation is found by the following formula:

$$\sigma = [\Sigma(x_i-\mu)^2/N]^{1/2} \qquad \text{(Equation 3)}$$

The same process was repeated for each time period for each location for each year, and for each solar minimum and maximum for each year.

To further explain average and standard deviation, here is a sample calculation. Suppose one wants to find the average and standard deviation of the following four numbers: 1.25, 2.00, 1.42, and. 2.25.

$$\text{Average} = (1.25 + 2.00 + 1.42 + 2.25) / 4$$

$$= 1.73$$

Solar Cycle

For the solar cycle part of the project, I found an internet table at ftp://ftp.ngdc.noaa.gov/ that was referenced for each month's sunspot number. The number of sunspots can be used as a proxy for the level of solar activity and position in the solar cycle. The average sunspot numbers for each season of each year was calculated and recorded in Table 12 in Chapter 4. These calculated numbers will be discussed in future chapters for their relevance to the seasonal and yearly data analyzed.

Access Program

Access was used to delete erroneous data and import the large amounts of data into Matlab. (See Appendix A) Once corrected, the entire location's year of data is imported into a large database. These were renamed with monikers such as "Ancon98", depending on the location and year. Each database was then run through a query to eliminate S4, or Field 4, data that was greater than one. This was done because valid S4

values are only between the values of zero and one. Any values greater than one are assumed to be errors in the data. A second query was then run to separate the remaining good data into months of the year.

A third query was conducted for each hour at each location for each year. For example, a new file would be named "Ancon9800" to signify it contained all of hour zero's data from Ancon for year 1998. Since the time listed in the data is Universal Time (UT), and recorded in seconds, it was necessary to determine the hours of the day in seconds. (see Table 3 below)

Table 3. Hourly Time Table

Universal Time Table		
Hour	Start Second	End Second
0	0	3600
1	3600	7200
2	7200	10800
3	10800	14400
4	14400	18000
5	18000	21600
6	21600	25200
7	25200	28800
8	28800	32400
9	32400	36000
10	36000	39600
11	39600	43200
12	43200	46800
13	46800	50400
14	50400	54000
15	54000	57600
16	57600	61200
17	61200	64800
18	64800	68400
19	68400	72000
20	72000	75600
21	75600	79200
22	79200	82800
23	82800	86400

By using Table 4 above, I could find a trend in the data based upon the time of day. Since the time was recorded in UT, each location is a deviation from Greenwich Mean Time, or Universal Time. This will allow us to compare the different locations and still refer to the same hour in all locations. (see Table 4 below)

Table 4. Location Hourly Deviations

Location	Deviation from GMT (hours)
Ancon	-5
Antofagasta	-4
Asccension	0
Bahrain	3
Cuiaba	-4
Darwin	9.5
Diego	6
Fang	7
Guam	10
Manila	8
Marakparak	0
Parepare	8
Pontianak	7
Singapore	8
Vanimo	10

MatlabPlots

After trying to make a geomap with Grid Analysis and Display System, or GrADS, a new Matlab program was created and used to find differences between a solar minimum day and a solar maximum day. First, Access was used to find the day in 1998, our solar minimum year, that had the least activity and had the lowest S4 values. The same process was done for 2001, which is our solar maximum year. The solar minimum day was day 41 for year 1998 as recorded at Ancon, Peru. The solar maximum day was day 218 for year 2001 as recorded at Ancon, Peru. Each of these days was separated into each hour's data. For example, hour 01 had three text files made: hr01lat.txt (latitude),

hr01lon.txt (longitude), and hr01s4.txt (S4 data). These were loaded into a Matlab program that plotted the points onto a map of the world.

Summary

After receiving the scintillation data, a FORTRAN program used to put the year, day, time, S4, satellite latitude, and satellite longitude into one large matrix. Then this matrix was imported by year into Access database program. Queries were run to sort each location's data into months and hours of the day. The resulting files were then loaded into Matlab and each year and each season's average and standard deviation was found. Due to lack of time, only Antafagasta's diurnal, or hourly, data is presented in the next chapter. Finally, all of the season's data was put into a second Matlab program, and then a Matlab program geomapped the data on a map of the world.

IV. Results

After completing all of the procedures necessary for this project, each location's results were compiled. Each of the season's data will be presented here, and their relevance will be discussed in the following section.

General Location Information

All eleven of the Global Positioning System receiver stations are located near the equator, but their exact location determined the severity of scintillation. Three locations are in the Northern Hemisphere, four are in the Southern Hemisphere, and the remaining four are at the equatorial region of the earth. Each location's exact location on the globe can be seen in the table below. (See Table 5 below)

Table 5. Latitude and Longitude of GPS Receiver Locations

Location	Latitude	Longitude
Ancon	11 S	77 W
Antofagasta	23 S	70W
Asccension	7 S	14 W
Bahrain	27 N	81 E
Cuiaba	15 S	56 W
Darwin	12 S	130 E
Diego	34 S	59 W
Fang	19 N	99 E
Guam	13 N	144 E
Manila	14 N	121 E
Marakparak	5 S	120 E
Parepare	4 S	119 E
Pontianak	0 S	109 E
Singapore	1 N	103 E
Vanimo	2 S	141 E

Bahrain, Fang, and Guam are three of the eleven locations that are in the Northern Hemisphere. Antofagasta, Ancon, Ascension Island, and Diego Garcia Island are four of

the eleven locations that are located in the Southern Hemisphere. Darwin Island, Pontianak, Marak Parak, and Vanimo are the four of the eleven locations that are in the equatorial region of the world.

Seasonal Results

January to March

Location	*Jan-Mar Average*	*St. Dev.*
Antofagasta	0.0875	0.0071
Guam	0.081	0.01285
Asc. Island	0.0745	0.01169
Ancon	0.0877	0.00273
Bahrain	0.087	0.01236
Darwin	0.0572	0.0172
Diego	0.1164	0.00978
Fang	0.1263	0.1422
Marak Parak	0.0914	0.0802
Pontianak	0.069	0.0718
Vanimo	0.1479	0.0811

Overall: Average = 0.0933
Standard Deviation=0.0408

April to June

Table 7. April-June Results

Location	*Apr-Jun Average*	*St. Dev.*
Antofagasta	0.053	0.01
Guam	0.112	0.00953
Asc. Island	0.0721	0.00217
Ancon	0.0734	0.00377
Bahrain	0.0947	0.0055
Darwin	0.054	0.0153
Diego	0.1135	0.01269
Fang	0.1113	0.1287
Marak Parak	0.1167	0.0927
Pontianak	0.0758	0.0872
Vanimo	0.1412	0.1169

Overall: Average = 0.0925
Standard Deviation=0.044

July to September

Table 8. July-Sept Results

Location	*Jul-Sep Average*	*St. Dev.*
Antofagasta	0.0512	0.0108
Guam	0.121	0.01239
Asc. Island	0.0793	0.02058
Ancon	0.0693	0.00538
Bahrain	0.0826	0.00476
Darwin	0.06	0.00981
Diego	0.1032	0.00585
Fang	0.12	0.1959
Marak Parak	0.1292	0.06428
Pontianak	0.0791	0.0884
Vanimo	0.1606	0.1256

Overall: Average = 0.0923
Standard Deviation=0.049

October to December

Table 9. October-December Results

Location	*Oct-Dec Average*	*St. Dev.*
Antofagasta	0.0803	0.0032
Guam	0.0965	0.01115
Asc. Island	0.1174	0.00128
Ancon	0.078	0.0024
Bahrain	0.081	0.00639
Darwin	0.075	0.00934
Diego	0.112	0.00852
Fang	0.1125	0.1372
Marak Parak	0.1336	0.1047
Pontianak	0.0726	0.0758
Vanimo	0.1579	0.0988

Overall: Average = 0.1015
Standard Deviation=0.0423

Each location had a different S4 average scintillation maximum, but all but four of the eleven locations had their maximum between October and March. Antofagasta, Ancon, Diego, and Fang, had an average S4 scintillation peak in the months between Januaary and March. Only Bahrain had an average S4 scintillation peak during the months of April, May and June. Guam, Pontianiak, and Vanimo saw an average S4 scintillation peak in July, August and September. Ascension Island, Darwin, and Marak Parak all had their highest average S4 number between October and December. Between the months October and March, there is an increased S4 scintillation present. October to December has the largest amount of average S4 scintillation with 0.1015 and a standard deviation of 0.423.

First, each season was analyzed for its scintillation trends. The largest values of scintillation occurred during the months of October until March. The values ranged from 0.1015 during these peak months. During the rest of the year, the values were between 0.0423. While this trend is consistent with the findings of Bishop, Groves, and other researchers, I was surprised to find such low values. S4 scintillation is a zero to one range value, but with the current data a low value makes sense. All of the data was recorded between the hours of 2200 and 0700 Greenwich Mean Time. This means a large amount of spread F is present for half of the time, and not for the other half that is after 0000 GMT. Averaging such data will only give the user a basic idea of seasonal trends, and not the presence of spread F.

Yearly Results

Each year's data was averaged and compiled into the following table. The average and standard deviation was found, and then they were put into a graph to show yearly trends for scintillation S4 number. (see Table 10 and Figure 4 below)

Table 10. Yearly Trends

Year	Average	St. Dev.
1998	0.0287	0.03
1999	0.0583	0.0729
2000	0.0815	0.0866
2001	0.0863	0.0700
2002	0.0728	0.073
2003	0.0577	0.0919
2004	0.0466	0.0695

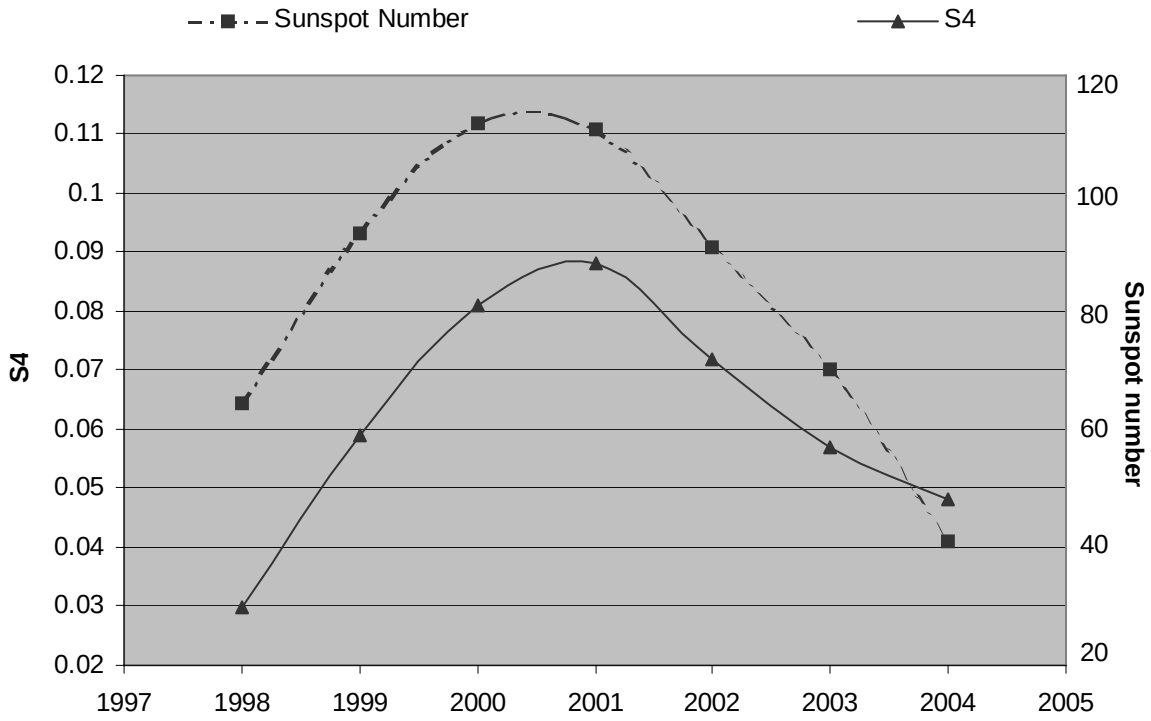

Figure 4.Yearly Trends

Hourly Results

Each location only had hourly data for hours zero thru seven GMT in the morning, and hours 2200 GMT and 2300 GMT at night, so only these hours could be analyzed. Due to time constraints, only Antofagasta's hourly data was compiled and averaged. (see Table 11 and Figure 5 below)

Table 11. Hourly Average

Hour (GMT)	Average
0	0.00597
1	0.0885
2	0.0953
3	0.0923
4	0.0801
5	0.0629
6	0.0524
7	0.048
22	0.0469
23	0.0466

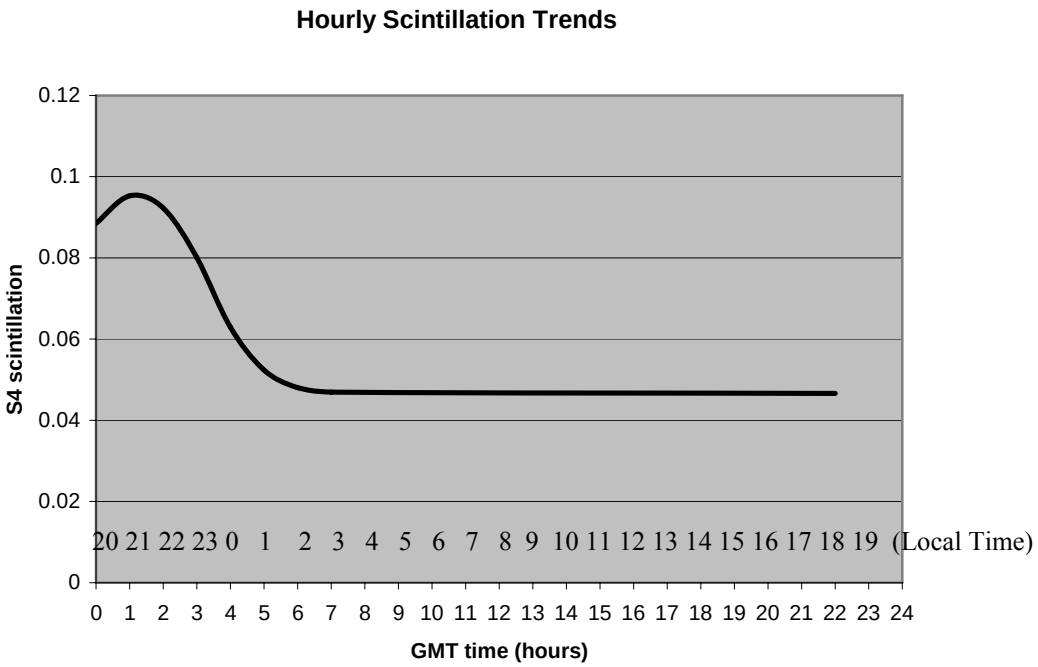

Figure 5. Hourly Scintillation Trends

Sunspot Yearly Averages

The sunspot numbers for each year were found recorded in the table below. (www.noaa.com) (see Table 12 below)

Table 12. Sunspot Numbers

Year	Annual
1997	21.5
1998	64.3
1999	93.3
2000	119.6
2001	110.9
2002	104.1
2003	63.6
2004	40.5
Average	77.2

Matlab Plots

Ancon, Year 2001, Day 41 (Solar Maximum, Active Day)

Hour 2200 GMT (5pm Local Time)

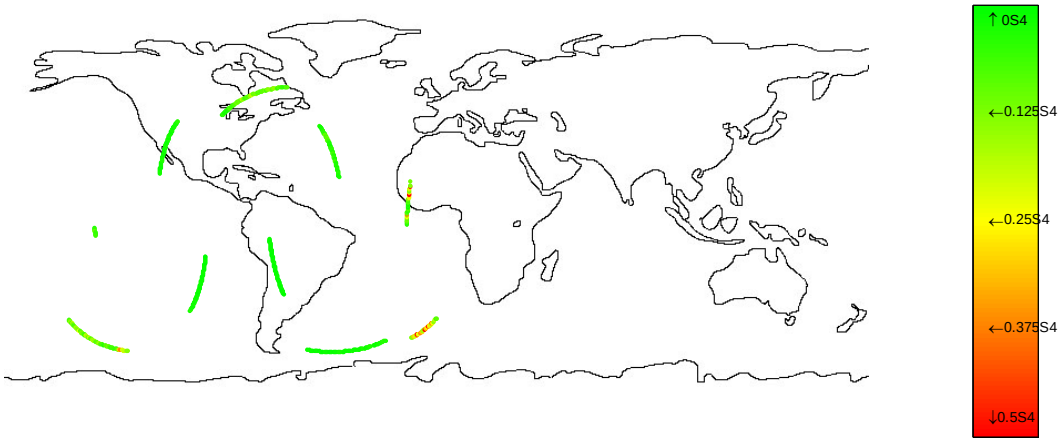

Figure 6. Ancon 2001 Day 41 Hr 2200

Hour 2300 GMT (6pm Local Time)

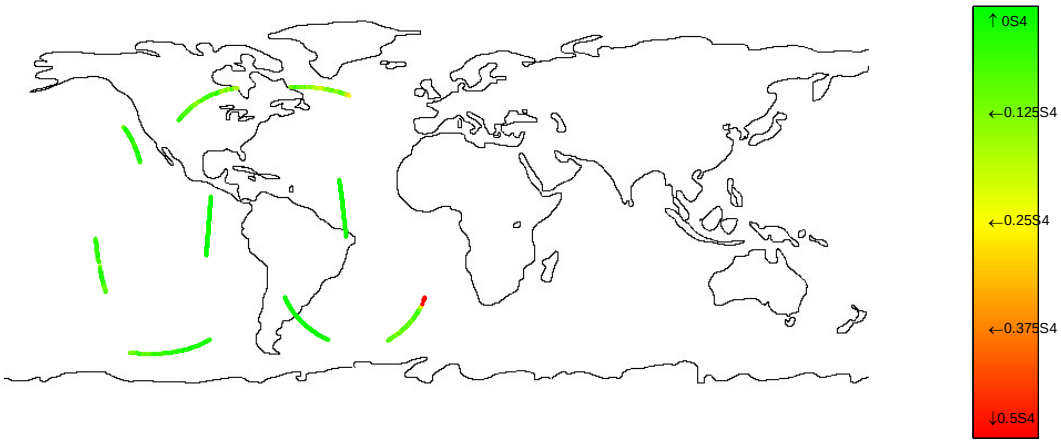

Figure 7. Ancon 2001 Day 41 Hr 2300

Hour 0000 GMT (7pm Local Time)

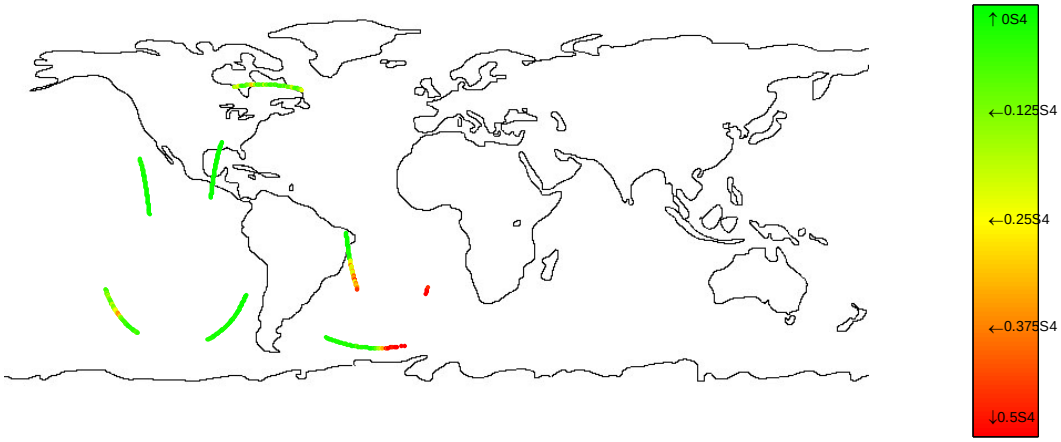

Figure 8. Ancon 2001 Day 41 Hr 0000 GMT

Hour 0100 GMT (8pm Local Time)

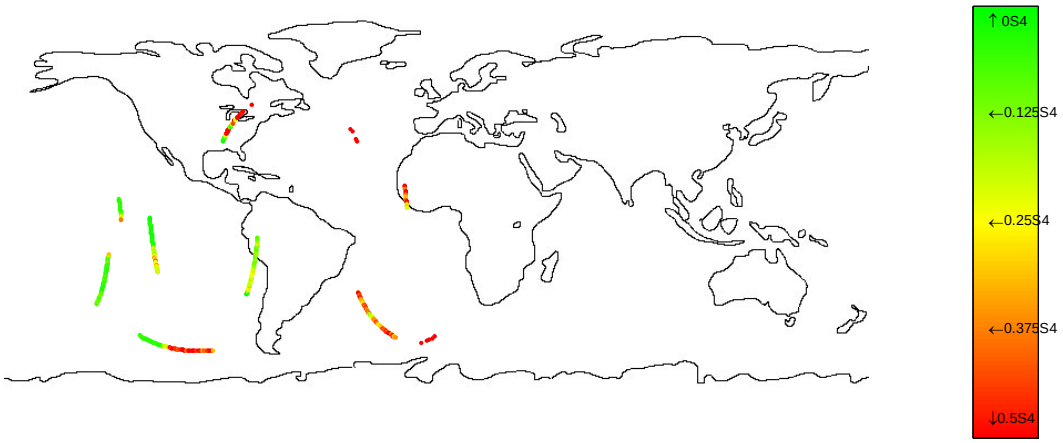

Figure 9. Ancon 2001 Day 41 Hr 0100 GMT

Hour 0200 GMT (9pm Local Time)

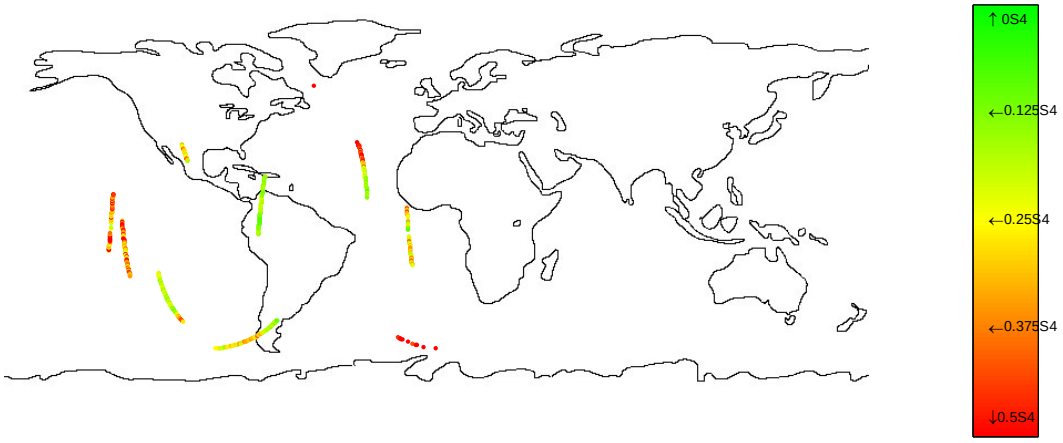

Figure 10. Ancon 2001 Day 41 Hr 0200 GMT

Hour 0300 GMT (10pm Local Time)

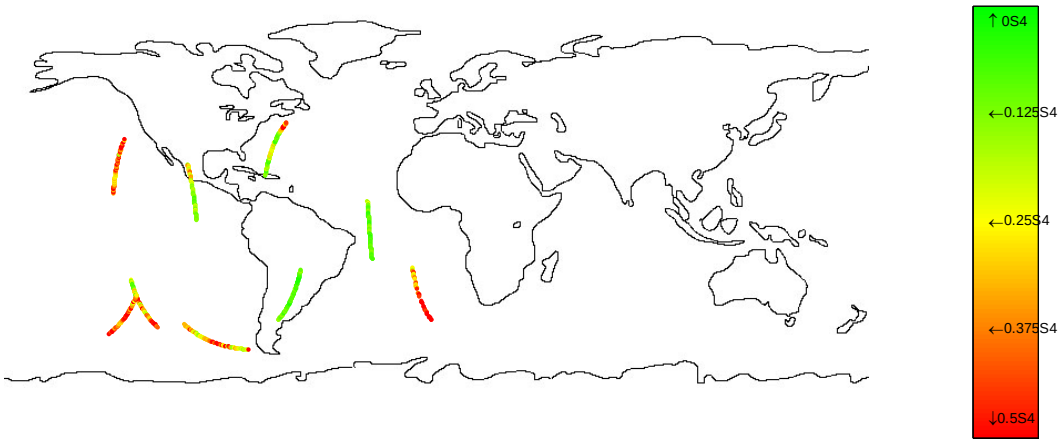

Figure 11. Ancon 2001 Day 41 Hr 0300 GMT

Hour 0400 GMT (11pm Local Time)

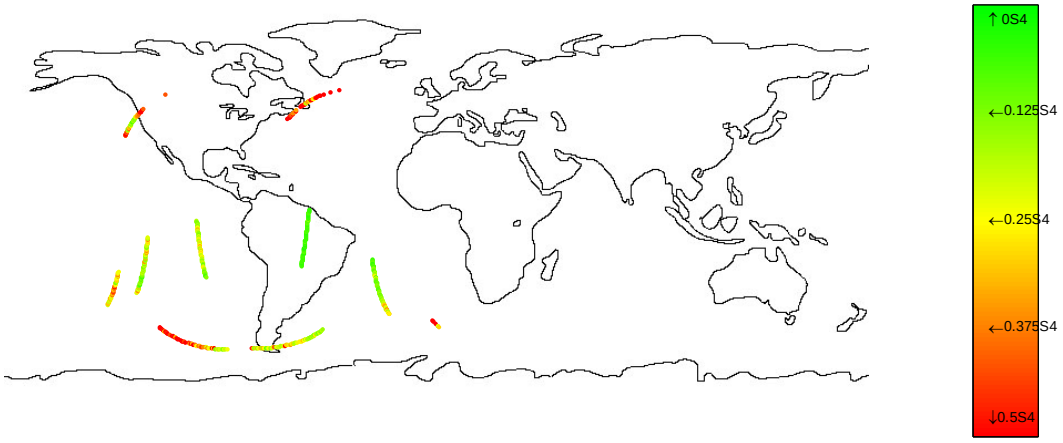

Figure 12. Ancon 2001 Day 41 Hr 0400 GMT

Hour 0500 GMT (12am Local Time)

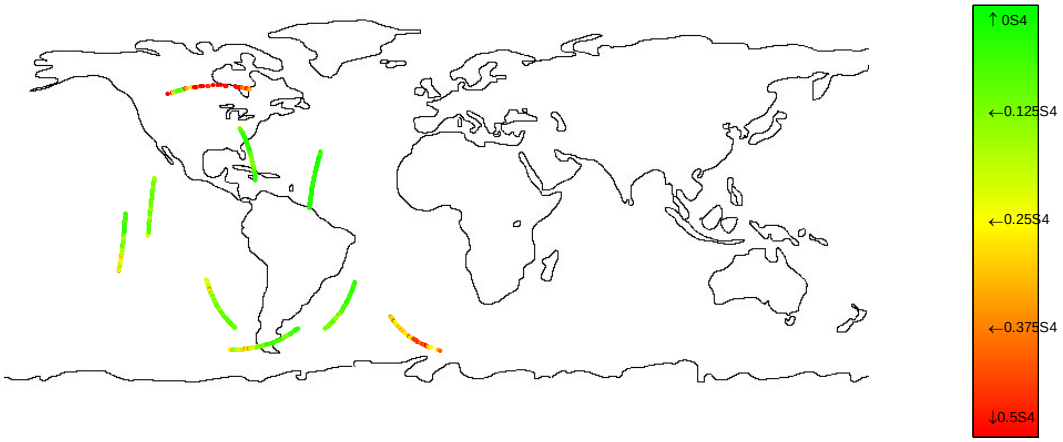

Figure 13. Ancon 2001 Day 41 Hr 0500 GMT

Hour 0600 GMT (1am Local Time)

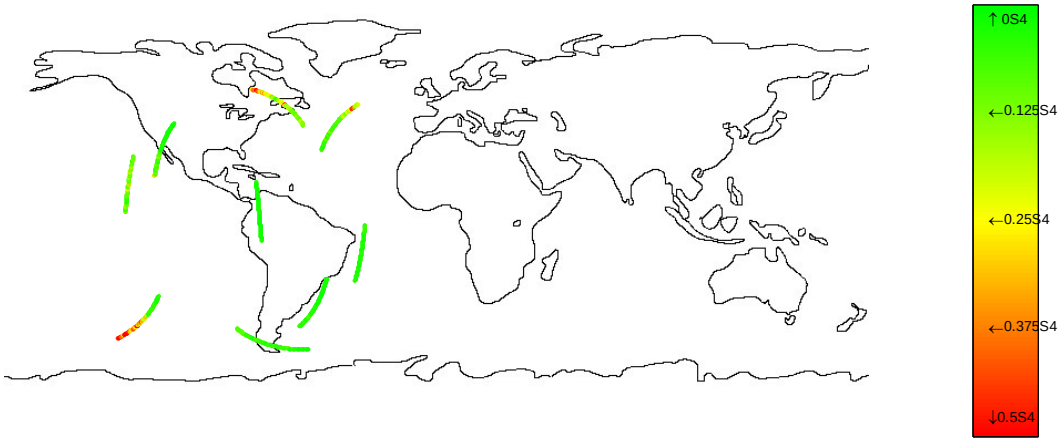

Figure 14. Ancon 2001 Day 41 Hr 0600 GMT

Hour 0700 GMT (2am Local Time)

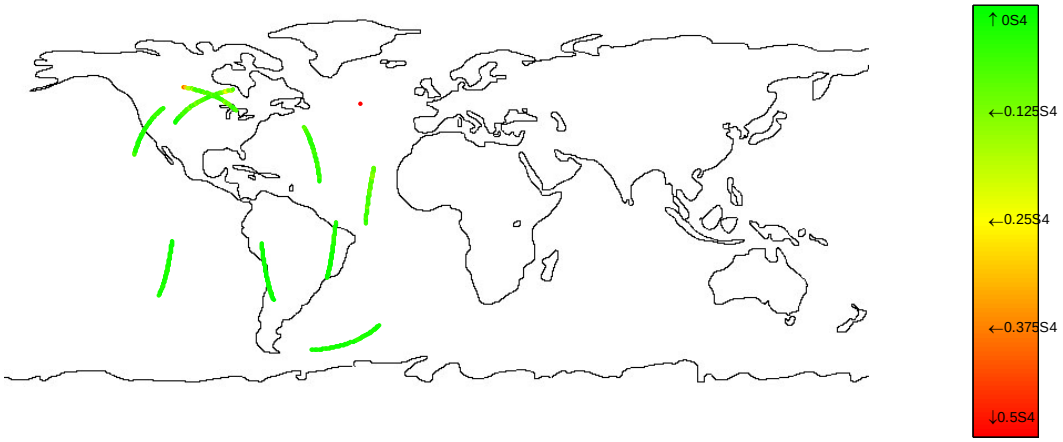

Figure 15. Ancon 2001 Day 41 Hr 0700 GMT

Ancon, Year 1998, Day 218 (Solar Minimum, Non-active Day)

Hour 0000 GMT (7pm Local Time)

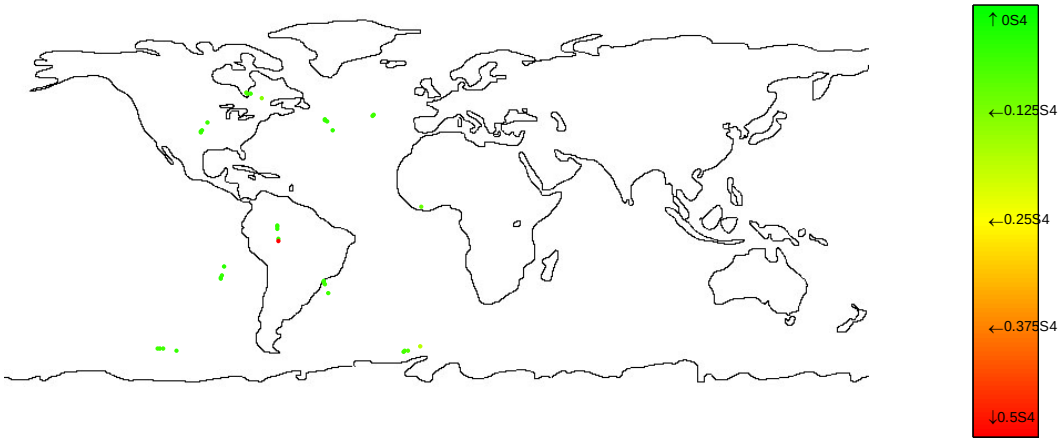

Figure 16. Ancon 1998 Day 218 Hr 0000 GMT

Hour 0100 GMT (8pm Local Time)

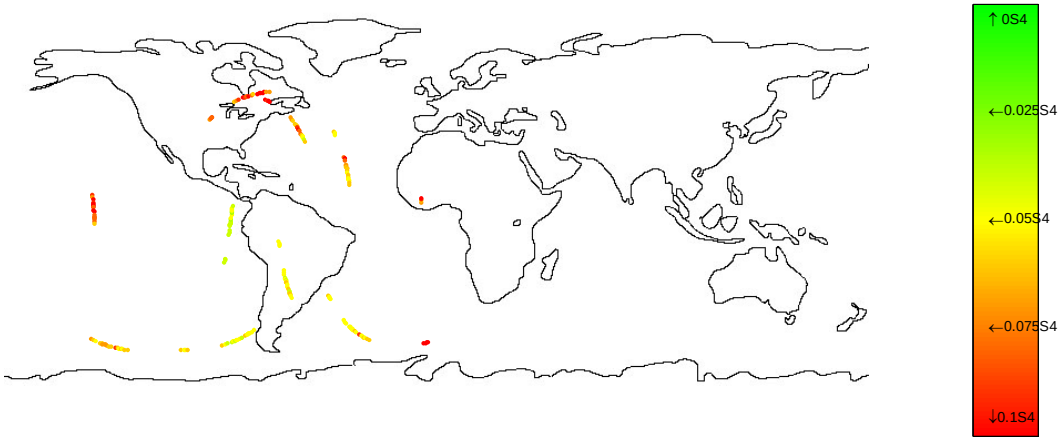

Figure 17. Ancon 1998 Day 218 Hr 0100 GMT

Hour 0200 GMT (9pm Local Time)

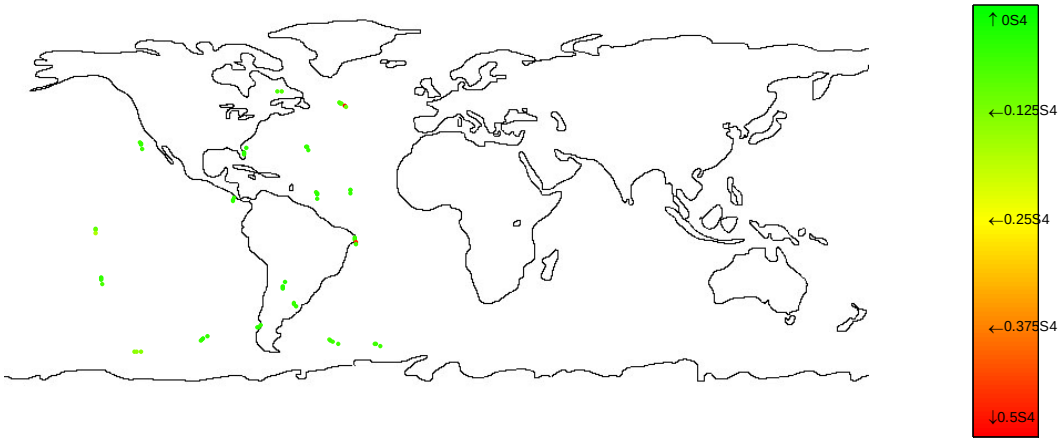

Figure 18. Ancon 1998 Day 218 Hr 0200 GMT

Hour 0300 GMT (10pm Local Time)

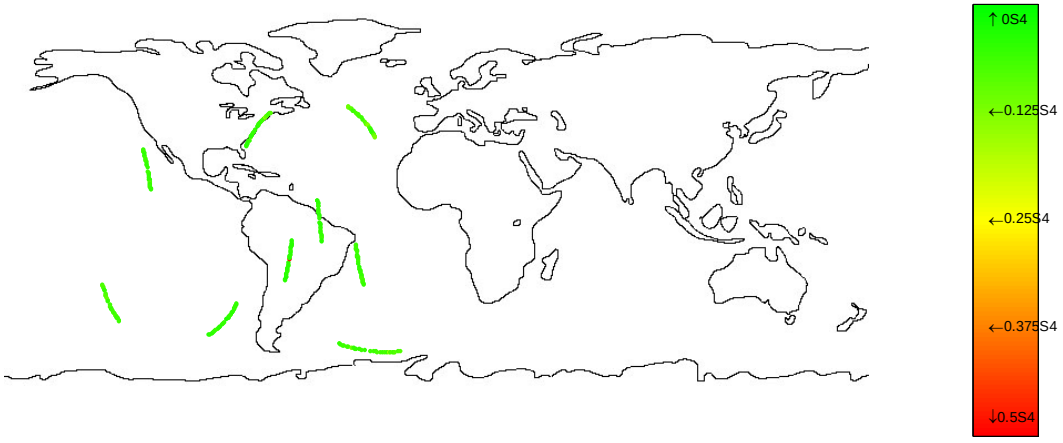

Figure 19. Ancon 1998 Day 218 Hr 0300 GMT

Hour 0400 GMT (11pm Local Time)

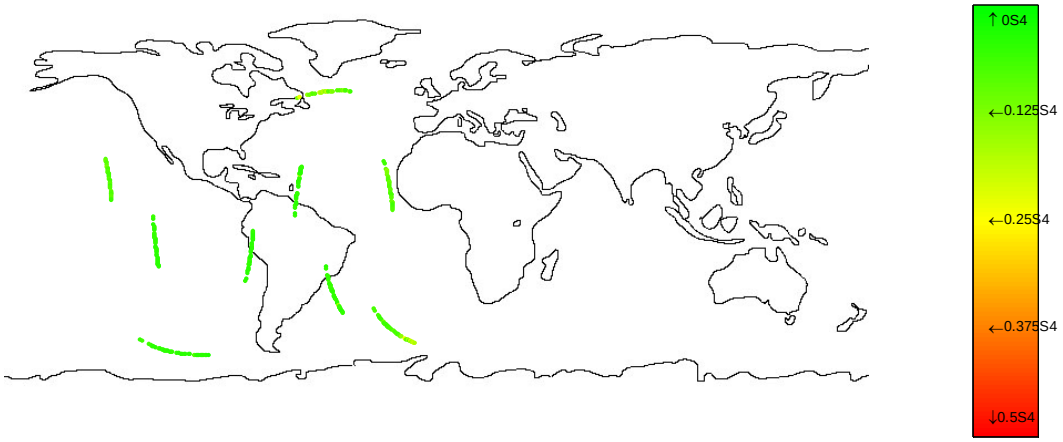

Figure 20. Ancon 1998 Day 218 Hr 0400 GMT

Hour 0500 GMT (12am Local Time)

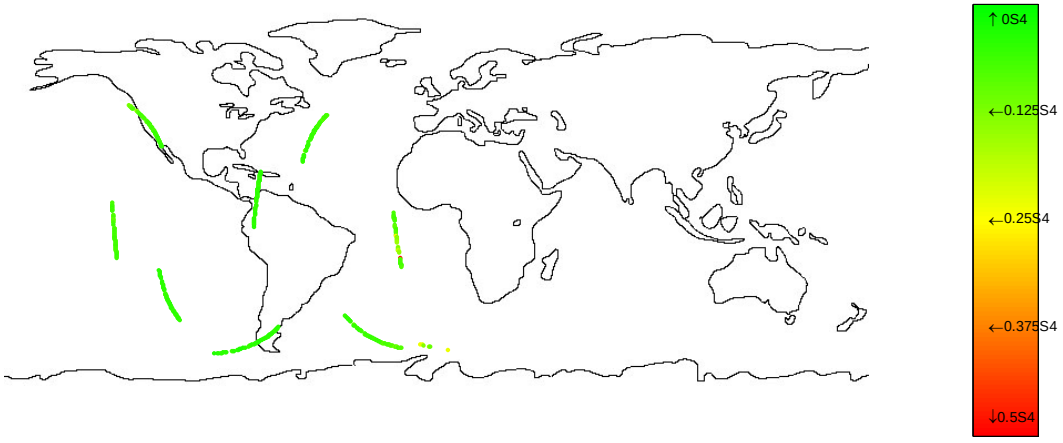

Figure 21. Ancon 1998 Day 218 Hr 0500 GMT

Hour 0600 GMT (1am Local Time)

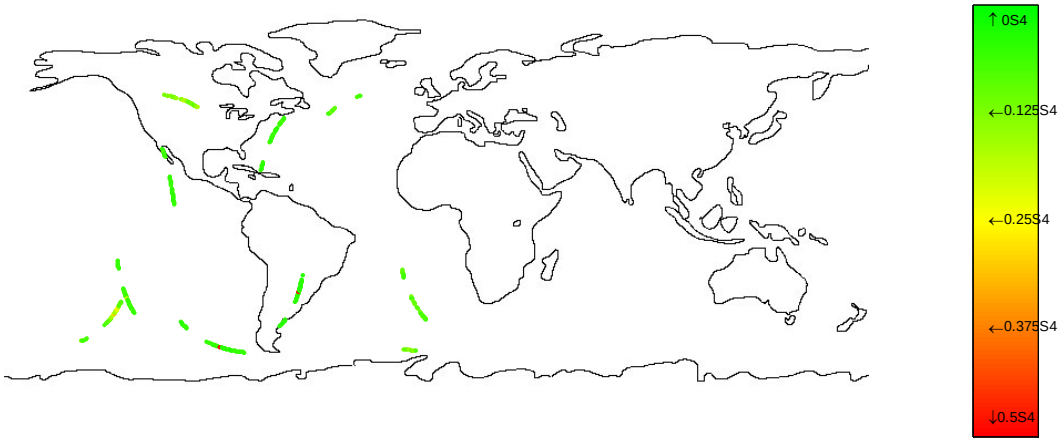

Figure 22. Ancon 1998 Day 218 Hr 0600 GMT

Hour 0700 GMT (2am Local Time)

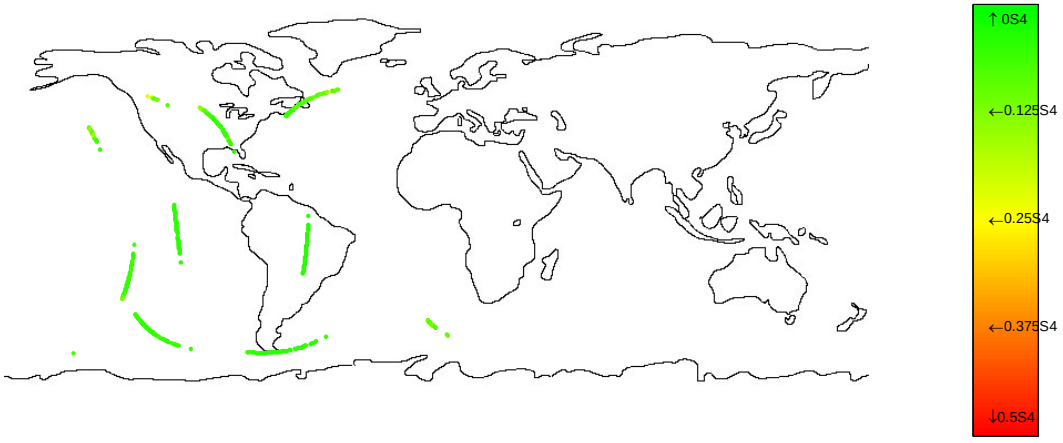

Figure 23. Ancon 1998 Day 218 Hr 0700 GMT

Summary

In summary, by running all the necessary computer programs, I have found trends based upon season, year, and hour. Seven of the eleven sites had their highest scintillation between the months of October and March, with October, November, and December having the highest average S4 numbers. By calculating the averages of the years, 1998 is shown to have a lower average scintillation than 2001. The yearly averages are also seen to follow the sunspot number cycle. By plotting the hourly data, it can be seen that between 2100 and 2300 local time (0100 and 0300 GMT), Antofagasta has the greatest average scintillation. It should also be noted here again that the data only recorded between the hours of 2200 and 0700 GMT. Not all locations had all these hours recorded, as can be seen in the Matlab plots. With the Matlab plots, it is clear that the non-active day in 1998 has less S4 scintillation present as compared to the active day in 2001.

V.Conclusions

After months of research, many new conclusions have formed. First, the seasonal trends agree with previous researchers that October to March is the time of most severe scintillation. Second, as the solar cycle reaches a maximum, the yearly S4 scintillation average also reaches a maximum. Third, the average scintillation at the equator peaks a few hours after midnight local time, and then proceeds to decrease in the morning hours following. Fourth, Matlab maps can be used predict the regions are seasons of most scintillation. More research in the area of maps will become useful to researchers and GPS users alike.

The seasonal peak in S4 scintillation can be attributed to the spread F anomaly and the equatorial electrojet. Spread F is caused by turbulence in the ionosphere, which in turn causes creates more plasma bubbles. An increase in ionospheric plasma bubbles means a more disturbed path for a radio signal, or increased scintillation. Spread F peaks at midnight and then rapidly falls in the following hours.

All but four of the eleven sites had their maximum S4 average during the months of October to March. The yearly averages saw an increase as the years reached solar maximum in 2001. The lowest S4 average was during solar minimum in 1998, and only increased as the years reached 2001. Then the average scintillation began to decrease until the data ended in 2004. The hourly trends saw a peak between the hours of 2100 and 2300 local time, which agrees with previous findings. As stated before, the most S4 scintillation is usually found between the hours after sunset and midnight local time. The

Matlab plots were created after a failed attempt at creating a feasible set of GrADS maps. While these do show the path of the satellite better than the GrADS, the exact location of the S4 scintillation is still unknown. The scintillation is recorded by the satellite according the satellite's position at that time. This tells us where the satellite is, and not where the actual scintillation may be present. These maps do show us that by comparing a solar minimum, non-active day to a solar maximum, active day, we can see a difference. The solar minimum day had less S4 scintillation present over the entire day than the solar maximum day. These maps also demonstrate the hourly peak first noted in the Antofagasta data. Both years saw a peak in scintillation between sunset and midnight, which agrees with previous findings.

Seasonal Trends

As the solar sunspot number increased from a solar minimum year in 1998 to a solar maximum year of 2001, the yearly S4 number increased. In 1998, the average scintillation S4 number was 0.0287 with a standard deviation of 0.03. In 2001, the average S4 number was 0.0863 with a standard deviation of 0.07.

Based upon the location of the receiver locations, many researchers have found similarities in the scintillation values. The seasonal trends for the Northern Hemisphere are shown in Table 13 and Figure 24. In this hemisphere, Bahrain and Guam have a similar basic trend, they do not match the trend found in Fang.

Table 13. Northern Hemisphere Averages

Northern Hemisphere				
Location	**Jan-Mar**	**Apr-Jun**	**Jul-Sep**	**Oct-Dec**
Bahrain	0.0861	0.0934	0.0838	0.08094
Fang	0.1263	0.1113	0.12	0.11252
Guam	0.0917	0.118	0.1244	0.09969

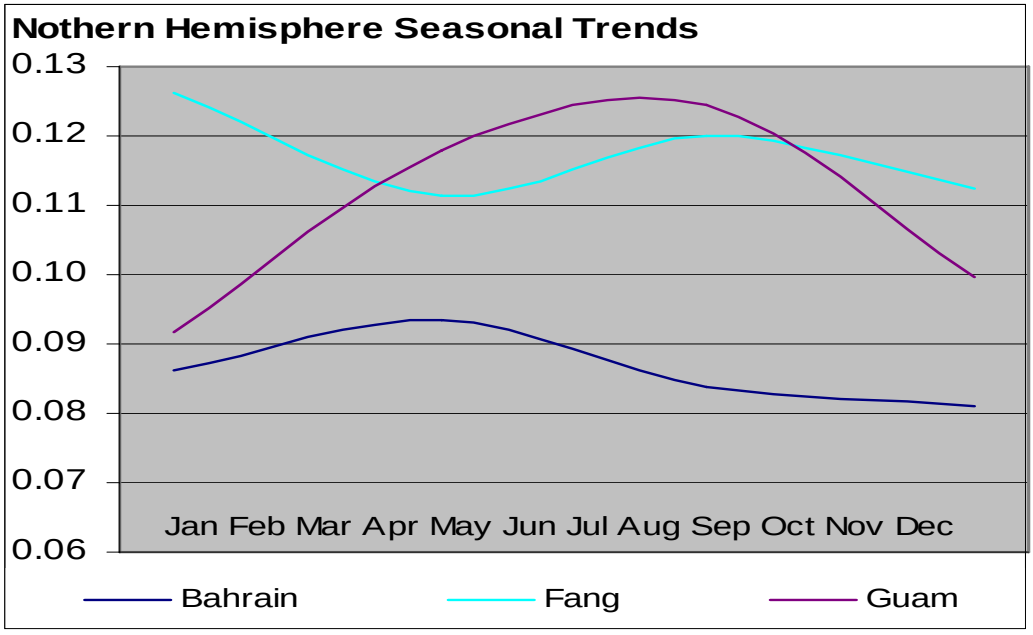

Figure 24. Northern Hemisphere Seasonal Trends

The seasonal trends for the equatorial region are displayed in Table 14 and 11. There is a general trend present that July, August and September has the highest average scintillation. This occurrence can be related to the higher average sunspot number during this time of the year, and the presence of the equatorial electrojet at these locations. Severe scintillation is present when the year in question is a solar maximum year in the eleven year solar cycle. Located at the equator, these locations are the most susceptible to scintillation effects.

Table 14. Equatorial Regions Averages

Equatorial Areas				
Location	**Jan-Mar**	**Apr-Jun**	**Jul-Sep**	**Oct-Dec**
Darwin	0.0629	0.0574	0.0611	0.07405
Pontinak	0.069	0.0758	0.0791	0.07266
Vanimo	0.1479	0.1412	0.1606	0.15785
Marak Parak	0.0914	0.1167	0.1292	0.13364

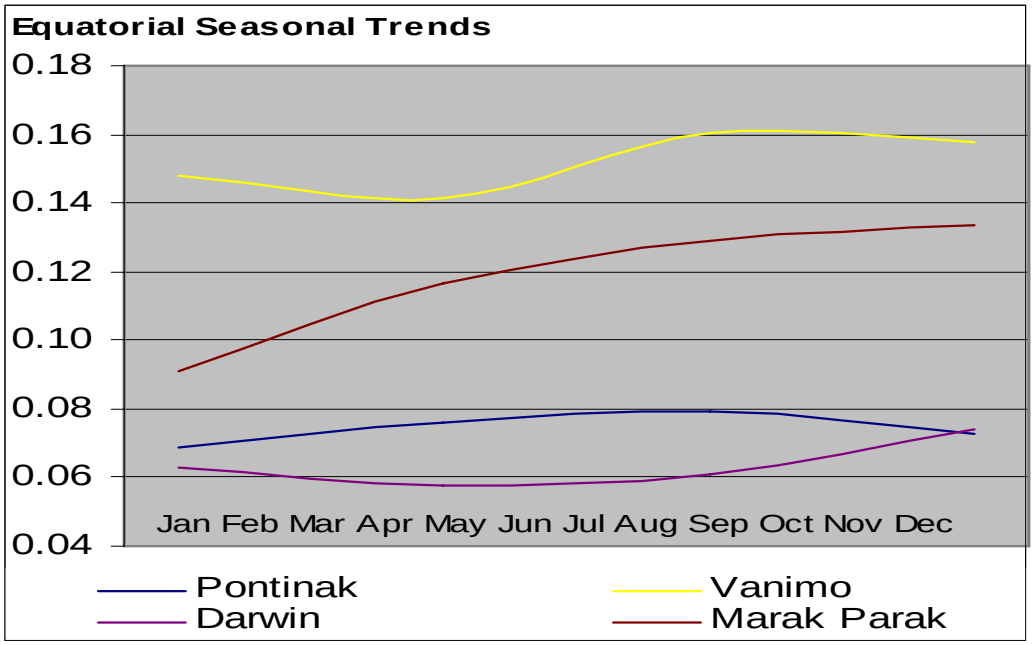

Figure 25. Equatorial Seasonal Trends

The southern hemisphere locations had a more definite trend than the northern or equatorial regions. Their seasonal trend results can be seen in Table 15 and Figure 26. These figures show that during the months of January thru March, and between October and December, the average scintillation is at its highest. The highest average is found in October, November and December when the earth is in its closest orbit to the sun. At this

time of the year, the planet is 5 million kilometers closer to the sun, allowing the earth to be more susceptible to a larger range of solar radiation. (see Figure 25 below) When solar radiation enters the ionosphere, more plasma bubbles are created and scintillation becomes more severe. The southern hemisphere is the only region that researchers focus on due to the wealth of receiver stations and data available. Our results support their findings that the worst scintillation is between the months of October and March.

Table 15. Southern Hemisphere Averages

Southern Hemisphere

Location	Jan-Mar	Apr-Jun	Jul-Sep	Oct-Dec
Antofagasta	0.0896	0.0586	0.0591	0.08594
Ancon	0.0877	0.0734	0.0693	0.07804
Ascension	0.0804	0.0614	0.0604	0.08478
Diego	0.1183	0.1159	0.1058	0.10913

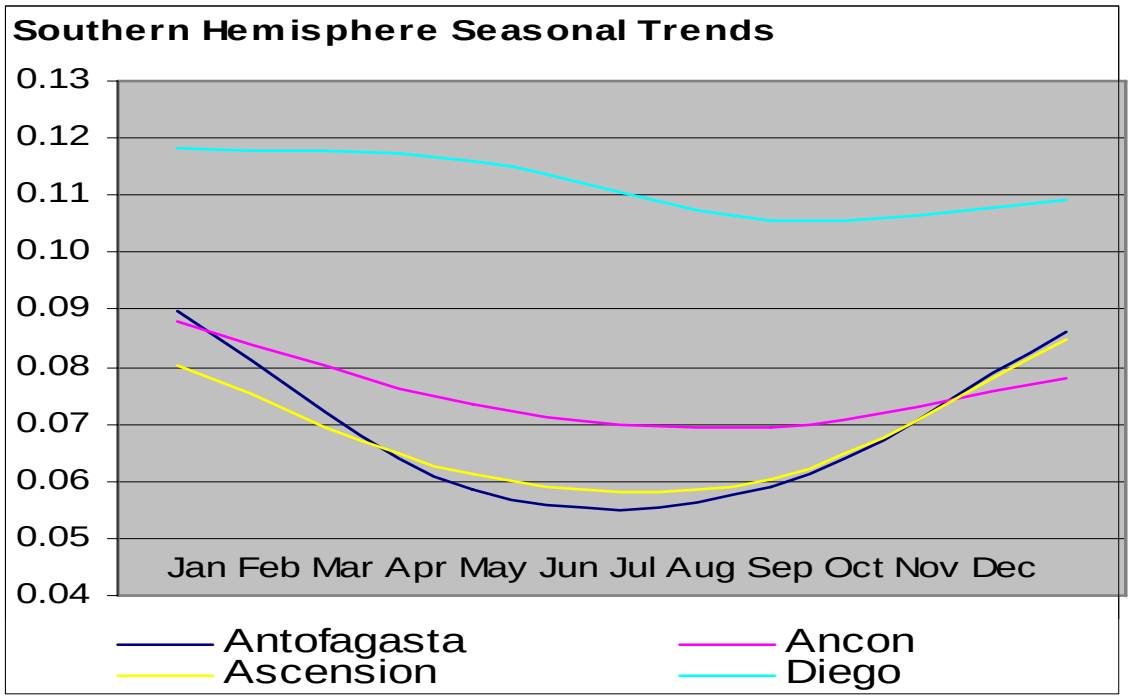

Figure 26. Southern Hemisphere Seasonal Trends

Table 16. Seasonal Trends Overview

Location	Jan-Mar	Apr-Jun	Jul-Sep	Oct-Dec
Ancon	0.09	0.07	0.07	0.08
Antofagasta	0.09	0.06	0.06	0.09
Ascension	0.08	0.06	0.06	0.08
Bahrain	0.09	0.09	0.08	0.08
Darwin	0.06	0.06	0.06	0.07
Diego	0.12	0.12	0.11	0.11
Fang	0.13	0.11	0.12	0.12
Guam	0.09	0.12	0.12	0.10
Marak Parak	0.09	0.12	0.13	0.13
Pontinak	0.07	0.08	0.08	0.07
Vanimo	0.15	0.14	0.16	0.16

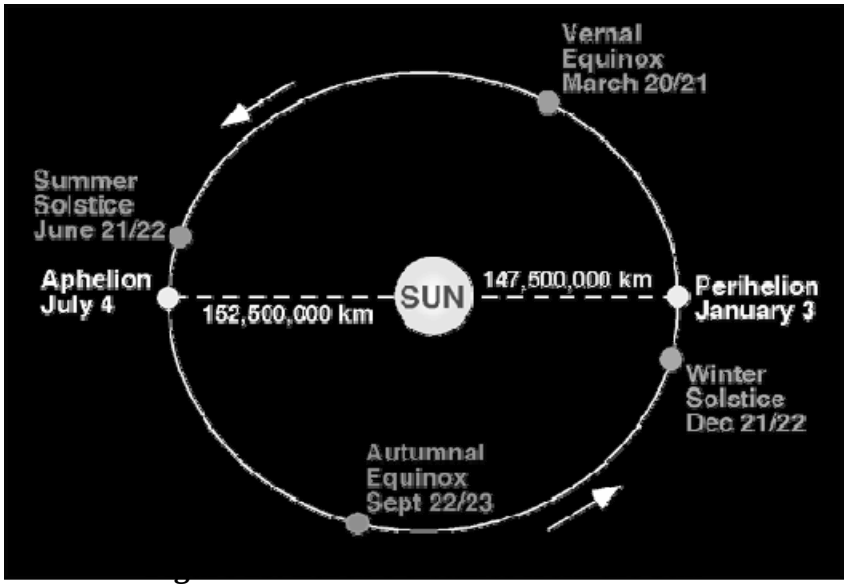

(from http://www.physicalgeography.net/fundamentals/6h.html)

Figure 27. Earth Orbit

For each season, or three-month interval, their average S4 scintillation and standard deviation numbers were calculated and presented in Chapter 4.

When the sun has a large number of sunspots present, the sun emits a larger amount of solar radiation towards the earth. At this solar maximum, the more solar radiation causes more plasma bubbles to form in the ionosphere. These bubbles are

formed by ionospheric plasma convection triggered by range spread F. When more bubbles are present, more irregularities are present, so the radio signals can become distorted. The intensity of solar radiation is directly proportional to the inverse of the squared distance of the earth to the sun. Therefore, every one percent decrease in distance from the earth to the sun equals a two percent decrease in solar radiation that reaches the earth.

Yearly Trends

Each year's average was found and those results can be seen in Table 10 in Chapter 4. Year 2001 and 1998 were found to be the highest and lowest averages, respectively. In 2001, a solar maximum year, the average sunspot number was 109, while in 1998, the number was 40. Thus, the yearly trends found that a high average sunspot number correlates to a high average scintillation number for the year in question. While previous researchers have concluded that scintillation is related to the solar cycle, and therefore the sunspot number, few have related it to any yearly trends. It seems quite obvious though, since 2001 was a solar maximum year that the year's average scintillation numbers would be just as high.

The solar minimum years saw lower scintillation values at the equatorial anomaly region than solar maximum years. This data is consistent with previous research that S4 scintillation increases as solar sunspot numbers increase. A solar maximum year has significantly more sunspots than a solar minimum year. Once every eleven years, one year is considered to be a solar maximum year.

Hourly Trends

As mentioned before, I was unable to complete all of the hourly data for each location. However, I will comment on Antofagasta's hourly results found in Table 11 in Chapter 4. At hour 0200 Greenwich Mean Time, the average scintillation is at its highest, and then slowly decreases until hour 0700 Greenwich Mean Time. Each location's data contained a gap from hour 0800 Greenwich Mean Time until hour 2100 Greenwich Mean Time, so no data analysis is available for this time period.

The diurnal occurrence that causes the greatest scintillation after sunset is due to range spread F. Range spread F is most prominent at equatorial regions between the hours of 2100 and 0200 local time. Basically, radio waves hit the disturbed, or scintillated, ionosphere, and the wave is returned at different altitudes. This return affects the range of the radio wave's signal, or how far the signal can travel. Range spread F is different from frequency spread F, which uses density gradients to bend the radio waves. This bending causes the frequency to change, or make multiple frequencies. (Tascione)

Researchers have shown that the most intense scintillation is after sunset until midnight local time. (Bishop) To determine what each hour is in local time, I referred to Table 5 in Chapter 4, and found Antafagasa is 4 hours off Greenwich Mean Time. This means that 0200 Greenwich Mean Time is really 2200 local time, so the peak in our data is right after sunset. Then the data stays at a peak until after midnight, or 0400 Greenwich Mean Time. At this time the scintillation is 0.0801, and by 0100 local time, the scintillation has dropped to 0.0629. After midnight, the scintillation begins to weaken rapidly until sunrise, when the average dropped from 0.0801 to 0.048, or decreased by half in only three hours.

The hourly trends present for Antofagasta agree with previous finding that range spread F is the culprit for local time scintillation. Between 20 and 60 degrees of the geomagnetic equator, little can be said for the causes of scintillation. All that is understood is that abrupt changes in the ionosphere can cause range spread F scintillation.

In order to know when scintillation will occur, one must know of ionospheric irregularities due to the ionosphere's plasma bubbles, sunset terminator, and geomagnetic anomalies. Regions of the world must also be found to respond to the sudden changes in the ionosphere's intensity of orientation. Then, one could predict when and where scintillation will occur. For the time being, many questions must still be answered, and more equatorial research must be conducted.

Matlab Plots

By making Matlab maps of a solar minimum day with limited activity and solar maximum day with great activity, some general conclusions can be formed. First, since all of the maps have the same scale of zero to 0.5 S4 scintillation numbers, we can compare the two days' data. The amount of 0.25 and above data during the solar maximum day, is greater than solar minimum day. Therefore, the solar minimum day has more data points that are less than 0.25. Solar minimum days have lower S4 values than solar maximum days, as can be seen in the Matlab maps. Since both days were separated according to each hour's data, these maps can also be compared to the hourly data from Antofagasta, as seen in Chapter 4. The hours between sunset and midnight local time have the greatest scintillation regardless of solar activity. This agrees with the findings from Antofagasta and previous researchers.

It should be noted future research of this project would have to deal with the complex geometry of the situation. The Matlab maps show where the satellite is when it records a scintillation value. This is not necessarily the location of the scintillation at that point in time. By using geometry, future researchers can determine the exact location of where the scintillation is when the satellite records it. Without this information, we cannot compare our findings to equatorial anomaly data that shows scintillation peaks in different locations.

Summary

After analyzing years of scintillation data collected at equatorial sites, many conclusions have formed. First, when the solar cycle is a maximum, the equatorial S4 scintillation is also at a peak for the yearly average. Second, the months of October until March see the largest amount of scintillation at the equatorial anomaly. Third, as the sun sets in these locations, the S4 number increases until it peaks at midnight and quickly dies off in the hours after the peak.

These seasonal, hourly, and yearly trends agree with the findings of Groves, Bishop, Basu and countless others. By using such trends, researchers can determine what causes the problems with their GPS systems. If one researcher knows the basic scintillation trends at the equatorial anomaly, they can determine if their problem is mechanical or atmospheric in nature. This can save a great deal of time and money by not sending missions out into the region when it is know they cannot communicate with anyone via their GPS system.

Appendix A

Matlab Program

```
>> load janfebmars4.txt
load janfebmarlat.txt
load janfebmarlon.txt
x=linspace(-91.3,64.2,200);
y=linspace(-56.2,55.9,200);
y=y';
ss=griddata(lon,lat,ss,x,y);
i=find(isnan(ss));
ss(i)=zeros(size(i));
save ss.dat ss /ascii
```

Access Data Sorting

First, each year's data was sorted into the eleven locations. Then each location's 1998, 1999, 2000, 2001, 2002, 2003, and 2004 data is individually imported into Access. Initially this created incorrect number configurations in some columns, or whole columns would be blank. After realizing, this was due to the lack of column width space, I used the advanced button on the import table to alter the widths. (see Table 16 below)

Table 16. Access Adjustments

Field	Start	Width
Year	1	2
Day	3	4
Time	7	7
S4	14	9
Latitude	23	9
Altitude	32	9
Longitude	41	9

Bibliography

1. Ionospheric and Atmospheric Remote Sensing, http://iono.jpl.nasa.gov/scint.html

2. Northwest Research Associates, Inc., Ionospheric Scintillation Prediction Pages, http://www.nwra-az.com/ionoscint/

3. Bishop G., Basu S., Holland E., and Secan J., "Impacts of ionospheric fading on GPS navigation integrity", *Proceedings of ION GPS-94,* Institute of Navigation, 577-585, 1994.

4. Nordwall B., "Atmospheric/multipath concerns for DGPS", *Aviation Week, 145,* 60-61, 14 October 1996.

5. Knight M. and Finn A., "The impact of ionospheric scintillations on GPS performance", *Proceedings of ION GPS-96,* Institute of Navigation, 555-564, 1996.

6. Aarons, J., Mendillo M., and Yantosca R., "GPS phase fluctuations in the equatorial region during solar minimum", *Radio Science, 32,* 1535-1550, 1997.

7. Bishop G., Basu S., Groves K., Smitham M., Lehnis K., Jacobs D., Gehred P., Howell D., Bainum G., and Goldizen D., "Upcoming ionospheric impacts on GPS at solar max - what do we know / what do we need?", *Proceedings of ION GPS-96,* Institute of Navigation, 595-604, 1996.

8. Kelley, M., Heelis, R., *The earth's ionosphere : plasma physics and electrodynamics*, San Diego : Academic Press, 1989.

9. Parkinson, Bradford W., Spilker, James J., *The global positioning system : theory and applications*, Washington D.C., American Institute of Aeronautics and Astronautics, 1996.

10. Devore, Jay L. , *Probability and statistics for engineering and the sciences*, Belmont, CA, Thomson-Brooks/Cole, 2004.

11. Groves, K., *Ionospheric scintillation and its effects on systems*, PowerPoint presentation, CISM Summer School, Boston University, 26 July – 6 August, 2004.

12. McHarg, G., AFIT Overview November 2004: Space Physics and Atmospheric Research Center, 17 Nov 04.

13. Air Force Research Laboratory, Space Vehicles Directorate, http://www.vs.afrl.af.mil

14. Thayer, J., "The convergence of magnetospheric energy flux in the polar atmosphere", *The Journal of Atmospheric and Solar-Terrestrial Physics,* 66, 807-824, 2004.

15. National Oceanic and Atmospheric Administration, www.noaa.com

16. Time and Date Calendars, http://www.timeanddate.com/calendar/

17. Datta-Barua, S., "Ionospheric Scintillation Effects on Single and Dual Frequency GPS Positioning", Institute of Nav., GPS/GNSS Meeting, Portland OR, Sept 2003.

18. Brown, A., "GPS Ionospheric scintillation measurements using a bean steering antenna array for improved signal/noise", NAVSYS Corp., ION Meeting, Denver, CO, June 1998.

19. Fu, W., "Real-Time Ionospheric Monitoring", 12th Int. Tech. Meeting of Satellite Division of the U.S. Institute of Navigation, GPS ION 99, Nashville, TN, Sept 1999, 1461-1471.

20. Thomas, R. M., "Statistics of GPS Satellite Links in the Presence of Equatorial Scintillation", Workshop on Applications of Radio Science, LaTrobe University, Australia, April 2000, 142-148.

21. Fundamentals of Physical Geometry, http://www.physicalgeography.net/fundamentals/6h.html

22. Tascione, Thomas F., *Introduction to the Space Environment,* Malabar, Florida, Krieger Publishing Company, 1988.

23. Hajkowski, "Fringe Effects in Mid-Latitude Scintillations over a Solar Maximum", Aberystwth, UK, University of Wales, 1994.

Vita

Lieutenant Katharine A. Wicker graduated from Loveland High School in Loveland, Ohio. She attended Bowling Green State University in Bowling Green, Ohio, where she participated in AFROTC at Detachment 620. She graduated with a Bachelor of Science in Biology, and received a commission into the United States Air Force to attend the Graduate School of Engineering and Management at the Air Force Institute of Technology is her first assignment. Upon graduation she will be attending Space and Missile training at Vandenberg AFB, California.

REPORT DOCUMENTATION PAGE	Form Approved OMB No. 074-0188

1. REPORT DATE *(DD-MM-YYYY)*	2. REPORT TYPE	3. DATES COVERED *(From – To)*
14 Mar 06	**Master's Thesis**	23 May 04 – 23 Mar 06

4. TITLE AND SUBTITLE

A Climatological Study of Equatorial GPS Data And the Effects on Ionospheric Scintillation

5a. CONTRACT NUMBER

5b. GRANT NUMBER

5c. PROGRAM ELEMENT NUMBER

6. AUTHOR(S)

Wicker, Katharine, A., 2nd Lieutenant, USAF

5d. PROJECT NUMBER

5e. TASK NUMBER

5f. WORK UNIT NUMBER

7. PERFORMING ORGANIZATION NAMES(S) AND ADDRESS(S)
Air Force Institute of Technology
Graduate School of Engineering and Management (AFIT/EN)
2950 Hobson Way
WPAFB OH 45433-7765

8. PERFORMING ORGANIZATION REPORT NUMBER

AFIT/GSS/ENP/06-02

9. SPONSORING/MONITORING AGENCY NAME(S) AND ADDRESS(ES)
Dr. Keith M. Groves
29 Randolph Road, Air Force Research Laboratory
Space Weather Center of Excellence, Space Vehicles Directorate
Hanscom AFB, MA 01731
(781)377-3137

10. SPONSOR/MONITOR'S ACRONYM(S)

11. SPONSOR/MONITOR'S REPORT NUMBER(S)

12. DISTRIBUTION/AVAILABILITY STATEMENT
APPROVED FOR PUBLIC RELEASE; DISTRIBUTION UNLIMITED

13. SUPPLEMENTARY NOTES

14. ABSTRACT

Ionospheric Scintillation is detrimental to radio signals, especially those from global positioning systems, or GPS. Such scintillation is caused when a signal permeates the ionosphere through plasma bubbles. The signal's phase and amplitude can be altered, and a receiver on the ground can lose lock on the GPS signal. Measured using an zero to one index known as S4, scintillation severity is based upon season, solar cycle, time of day, location and frequency. The most severe scintillation occurs at the equatorial anomaly, or fifteen degrees north and south of the equator. Seven years of data from fifteen different locations around the equator were put into a Matlab program to determine if the current trends still apply. Previous research has found the S4 at the equator to peak during the months of September to March, between the hours of 2000 and 0300 local time, and when the sunspot number is above 60. Matlab plots were generated to find peaks in scintillation based upon location and month. These were compared to an table to sunspot numbers during those months. A new Matlab program was made to compile all of the plots into a climatological map of the seasonal data. Trends similar to those found previously were discovered. S4 numbers peaked in the area of the anomaly, and between the months of October to March. As the sunspot number increased, the yearly average scintillation also increased. The hours of 2200 local time and 2400 local time also saw a peak in S4 scintillation, which agrees with previous findings.

15. SUBJECT TERMS
Ionospheric Scintillation, Global Positioning Satellite, Equatorial Anomaly, Equatorial Electrojet, Ionosphere, S4 Scintillation, Solar Minimum/Maximum, Ionospheric Seasonal Trends, Ionospheric Diurnal Trends, GrADS

16. SECURITY CLASSIFICATION OF:			17. LIMITATION OF ABSTRACT	18. NUMBER OF PAGES	19a. NAME OF RESPONSIBLE PERSON
REPORT	ABSTRACT	c. THIS PAGE			Lt. Col. Steve Fiorino
U	**U**	**U**	**UU**	66	**19b. TELEPHONE NUMBER** *(Include area code)* (937) 255-3636 x4506; e-mail: Steven.Fiorino @afit.edu